IN VIVO MOLECULAR IMAGING: LIGAND DEVELOPMENT AND RESEARCH APPLICATIONS

MASAHIRO FUMITA
AND ROBERT B. INNIS

In positron emission tomography (PET) and single-photon emission computed tomography (SPECT), tracers labeled with radioactive isotopes are used to measure protein molecules (e.g., receptors, transporters, and enzymes). A major advantage of these two radiotracer techniques is extraordinarily high sensitivity ($\sim 10^{-9}$ to 10^{-12} M), many orders of magnitude greater than the sensitivities available with magnetic resonance imaging (MRI) ($\sim 10^{-4}$ M) or magnetic resonance spectroscopy (MRS) ($\sim 10^{-3}$ to 10^{-5} M). For example, MRI detection of gadolinium occurs at concentrations of approximately 10^{-4} M (1), and MRS measures brain levels of γ-aminobutyric acid (GABA) and glutamine at concentrations of approximately 10^{-3} M (2,3). In contrast, PET studies with [^{11}C]NNC 756 in which a conventional bismuth germanate-based scintillator is used can measure extrastriatal dopamine D1 receptors present at a concentration of approximately 10^{-9} M (4). Because many molecules of relevance to neuropsychiatric disorders are present at concentrations of less than 10^{-8} $M,$ radiotracer imaging is the only currently available *in vivo* method capable of quantifying these molecular targets.

PET and SPECT quantify the distribution of radioactivities in the brain, the direct *in vivo* correlates of *in vitro* autoradiographic film techniques such as receptor autoradiography, Western blots, and Northern blots. Thus, the future possibilities of radiotracer imaging are broad and exciting—and include targets of receptors, signal transduction, and gene expression. From this broader perspective, PET and SPECT methodologies are described as ''*in vivo* molecular imaging.''

Although *in vivo* molecular imaging is a promising technique, several barriers— physical, monetary, and chemical—to its successful application in neuropsychiatric disor-

ders must be addressed. Physical barriers include limited anatomic resolution and the need for even higher sensitivity. However, recent developments with improved detector crystals (e.g., lutetium oxyorthosilicate) and three-dimensional image acquisition have markedly enhanced both sensitivity and resolution. (5). Commercially available PET devices provide resolution of 2 to 2.5 mm (6,7). Furthermore, the relatively high cost of imaging with SPECT, and especially PET, can be partially subsidized by clinical use of the devices. Recent approval of U.S. government (i.e., Medicare) reimbursement of selected PET studies for patients with tumors, epilepsy, and cardiac disease has significantly enhanced the sales of PET cameras and their availability for partial use in research studies. Thus, the major barriers for the expanded use of PET are not physical or monetary, but rather chemical in nature. Simply stated, the major barrier to radiotracer imaging of molecular targets may well be the difficulties associated with developing the radiotracers themselves. Labeling the appropriate precursor typically is not the major impediment. Almost all candidate ligands contain carbon and hydrogen, and the positron-emitting nuclides ^{11}C and ^{18}F can usually be incorporated as an isotopic variant (^{11}C for ^{12}C) or an atomic substitute (^{18}F for ^{1}H). As described in the next section, the most common obstacle to the development of *in vivo* tracers is the relatively small window of appropriate combinations of lipophilicity, molecular weight, and affinity. For a molecule to pass the blood–brain barrier, relatively small molecular weights, less than 400 to 600 daltons (d), and moderate lipophilicity are required. However, in brain, relatively low lipophilicity and high affinity are required to achieve high ratios of specific to nonspecific binding. In contrast, the requirements for *in vitro* ligands are much less stringent because the blood–brain barrier can be removed by homogenization or tissue sectioning and most nonspecific binding washed away. The special requirements of *in vivo* probes (low molecular weight, high affinity, and just the right amount of lipophilicity) are discussed in the next section.

Masahiro Fumita: Department of Psychiatry, Yale University School of Medicine, New Haven, Connecticut.

Robert B. Innis: Departments of Psychiatry and Pharmacology, Yale University School of Medicine, New Haven, Connecticut.

Blood-brain-barrier

FIGURE 31.1. Compartmental description of radioactively labeled tracer uptake in brain.

REQUIRED PROPERTIES OF AN *IN VIVO* TRACER

In addition to a high degree of affinity and selectivity, several other properties are required for useful *in vivo* tracers.

Combination of Small Molecular Weight, Appropriate Lipophilicity, and High Affinity

Tissue uptake of a drug (whether radioactive or not) is often analyzed within the theoretic framework of a *compartment,* which is defined as a space in which the concentration of a drug is uniform. Within brain tissue, the time-dependent concentration of drug is described for at least three compartments—free [$C_{2f}(t)$], nonspecifically bound [$C_{2ns}(t)$], and specifically bound [$C_3(t)$] radiotracer (Fig. 31.1). Free and nonspecifically bound ligand, $C_{2f}(t)$ and $C_{2ns}(t)$, cannot be washed away, the way they are in *in vitro* studies. Therefore, a high ratio of specific to nondisplaceable uptake in brain (C_3/C_2) is required to obtain reliable data; to reduce the number of unknown variables, $C_{2f}(t)$ and $C_{2ns}(t)$ are often combined in a single compartment and defined as a compartment, $C_2(t)$) (Fig. 31.2).

Blood-brain-barrier

FIGURE 31.2. Three-compartment model (two tissues). To reduce the number of variables, $C_{2f}(t)$ and $C_{2ns}(t)$ in Fig. 31.1 are combined in a single compartment, $C_2(t)$.

Three major factors (i.e., lipophilicity, molecular weight, and affinity) determine the *in vivo* characteristics of a tracer. It is easy to understand that small molecular weight and a high degree of lipophilicity are required to pass the blood–brain barrier because it is composed of a lipid bilayer. However, lipophilicity has opposing effects on the brain uptake of a tracer. Increasing lipophilicity enhances the permeability of the compound, but it also tends to increase plasma protein binding, thereby decreasing the concentration of free drug available to cross the blood–brain barrier. From rat experiments in which 27 tracers of various chemical classes were used, Levin (8) obtained the following simple equation to derive a capillary permeability coefficient, P_c, from an octanol/water partition coefficient, P, and the molecular weight, M_r.

$$\text{Log } P_c = -4.605 + 0.4115 \bullet \log[P(M_r)^{-1/2}]$$

This equation was obtained for the tracers with molecular weights of less than 400 and relatively low lipophilicity (average log P, -0.34; standard deviation, 2.3). Because a higher lipophilicity is required for brain imaging tracers to be taken up adequately in brain, the equation only partially characterizes capillary permeability. High lipophilicity (higher value of log P) increases the binding to the plasma components (protein and cell membranes) (9) and reduces the capillary permeability coefficient expressed relative to the total plasma concentration of drug (10,11). Therefore, both low lipophilicity and high lipophilicity decrease the penetration of imaging agents across the blood–brain barrier, so that a parabolic curve is created (Fig. 31.3).

Although low lipophilicity decreases nonspecific binding in brain, it also decreases blood–brain barrier permeability (11). For any particular chemical series, optimal parameters
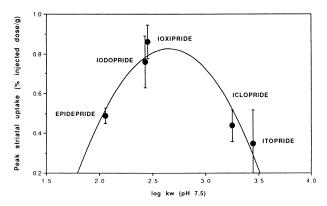

FIGURE 31.3. Relationship between apparent lipophilicity (log K_W) at pH 7.5 and peak striatal uptake (percentage of administered dose per gram of tissue in rat brain). Peak uptake occurred between log K_W of 2.4 and 2.8. Each point is the mean of four animals ± standard deviation. (From Kessler RM, Ansari MS, de Paulis T, et al. High-affinity dopamine D2 receptor radioligands. 1. Regional rat brain distribution of iodinated benzamides. *J Nucl Med* 1991;32:1593–1600, with permission.)

of affinity and lipophilicity generate a tracer with the best "signal-to-noise" ratio to measure the target molecule, as shown in Fig. 31.3 for a series of benzamide ligands for the dopamine D2 receptor. It should be noted that iodination for SPECT tracers usually increases lipophilicity in addition to molecular weight. Therefore, depending on the position in the optimization curve (Fig. 31.3), either an iodinated or a non-iodinated compound may show the most desirable *in vivo* properties.

Rapid Labeling of Precursor

The radionuclide must be incorporated quickly into appropriate precursor molecules because of the relatively short half-lives ($t_{1/2}$) of the isotopes (e.g., ^{11}C, 20.4 minutes; ^{18}F, 110 minutes; ^{123}I, 13.2 hours). Therefore, precursors must be available that allow quick labeling in one (but usually no more than two) synthetic steps just before the imaging study is performed.

Appropriate Clearance from Specific Binding Compartment

Following the bolus injection of radioactive tracer, the time–activity curve of an organ (e.g., brain) and its subcomponents (e.g., striatum) is characterized by uptake (rising) and washout (declining) phases. If the uptake phase is slow relative to the $t_{1/2}$ of the radionuclide, reasonably accurate data may be acquired only for the rising portion of the time–activity curve. Although parameters related to receptor density and affinity can be derived for selected targets with only the uptake portion, most quantitative methods calculate such parameters with both uptake and washout phases of the tissue time–activity curve. Thus, the tissue clearance of the tracer must typically be matched with the $t_{1/2}$ of the radionuclide. For example, ^{123}I can be used to quantify tracers with much slower tissue kinetics than ^{11}C. The rate of tissue clearance is in part determined by the affinity of the tracer, with ligands of higher affinity tending to "stick" longer to the target molecules. So, as with lipophilicity, the affinity of the candidate tracer should be high enough that significant tissue uptake occurs, but it should not be so high that washout is delayed beyond the usable measurement time of the radionuclide.

In summary, a low molecular weight is almost always mandatory, at least for tracers that cross the blood–brain barrier via passive diffusion. Lipophilicity should be high enough to allow adequate permeability of blood–brain barrier, but not so high as to cause unacceptable binding to plasma proteins or high levels of nonspecific binding in brain. Finally, the affinity of the tracer must balance the opposing goals of tight binding and fast washout from the brain. That is, a high affinity ligand is needed to provide high levels of tight binding of the ligand to the preceptor. However, if the binding is of such high affinity that the ligand shows negligible washout from the brain during the

course of a typical study, then the washout rate cannot be determined and critical kinetic data are unavailable to calculate receptor levels in the brain. Such parameters are not required for therapeutic agents (in which fast uptake may not be even helpful) or for *in vitro* tracers (in which most nonspecific binding can be washed away). For example, the nondisplaceable uptake of [^{18}F]haloperidol (12) and [^{11}C]cocaine (13) is unacceptably high for optimal PET imaging of their molecular targets, dopamine D2 receptor and dopamine transporter, respectively, although they can provide valuable data about the disposition of the psychoactive drugs themselves. It should also be noted that desirable properties of radioactive tracers are usually different from those of therapeutic agents. For, example, slow clearance of haloperidol from brain (12,14) may maintain effective receptor occupancy for a long period of time. If the distribution in the nonspecific binding compartment [$C_{2ns}(t)$ in Fig. 31.1] is large, the compartment may act as a reservoir of the drug and provide stable levels in brain. The stringent requirements for an optimal radioactive tracer easily explain why only a tiny percentage of *in vitro* tracers and therapeutic agents are useful as *in vivo* imaging ligands.

Negligible Influence of Radioactively Labeled Lipophilic Metabolites

If the parent tracer generates lipophilic radioactive metabolites, they may enter the brain in significant concentration and confound the imaging study. If they do not bind to the molecular target (inactive metabolites), they will increase nonspecific binding [$C_{2ns}(t)$ in Fig. 31.1] and thereby decrease the signal-to-noise measurement of the target. On the other hand, if the radioactive metabolites are active (i.e., bind to the target), quantification is highly confounded because the measured signal represents undetermined proportions of parent tracer and metabolite, each of which may have a different affinity for the target. The problem of lipophilic radioactive metabolites may sometimes be avoided by appropriate selection of the labeling position. For example, a tracer for the serotonin 5-HT$_{1A}$ receptor WAY 100635 can be labeled with ^{11}C at either an external (*O*-methyl) or internal (carbonyl) position. [*O*-methyl-^{11}C]WAY 100635 is rapidly metabolized in humans (15). The metabolic cleavage of WAY 100635 generates two moieties; the ^{11}C-containing methyl component is lipophilic and enters the brain, but the ^{11}C-containing carbonyl component is polar and does not enter the brain. The internal carbonyl labeling is more difficult than the external *O*-methyl labeling, but this clever radiochemistry has markedly improved the signal-to-noise measurement of 5-HT$_{1A}$ receptors in brain (16).

Many tracers currently used for imaging studies produce at least somewhat lipophilic metabolites. However, the quantities produced or their kinetics in passing blood–brain barrier are such that they do not commonly confound the measurements. For example, if the uptake and washout of the parent tracer are fast relative to the production of radio-

active metabolites, then their component of the total measured activity may be negligible during the imaging study.

IN VIVO QUANTIFICATION OF TRACER UPTAKE

In vivo quantification of molecular targets with radiotracer imaging is much more complicated than *in vitro* measurements for several reasons: (a) For *in vivo* experiments, tracers are intravenously administered and not directly applied to the target tissue. Therefore, the delivery of a tracer to the target tissue is influenced by its peripheral clearance (i.e., metabolism and excretion). (b) Total tissue activity is measured, and the separate specifically bound, nonspecifically bound, and free components (Fig. 31.1) are usually estimated with relatively complicated mathematical analyses. (c) The spatial resolution of cameras is limited, and the activity in a region of interest is influenced by tracer uptake in adjacent areas. The details of *in vivo* quantification are beyond the scope of this chapter, and interested readers should refer to other sources (e.g., refs. 17,18). The following section provides a simplified overview of the typical parameters and methods of quantification used in radiotracer imaging.

Binding Potential

In addition to having appropriate chemical and physical characteristics, a useful ligand must provide imaging results that are "amenable to quantification" because analogue/visual images are likely to be of limited utility in neuropsychiatric research. The most commonly measured receptor parameter is the binding potential (BP), which equals the product of receptor density (B_{max}) and affinity ($1/K_d$, where K_d is the dissociation binding constant). Thus, increased uptake could reflect either an increased number of receptors or the same number of receptors, each of which has a higher affinity for the ligand. To measure both B_{max} and K_d separately, at least two experiments or two injections are necessary, in which formulations of the tracer with both high and low specific activity are used (19,20). Because the injection of a tracer with low specific activity (i.e., high mass dose) causes significant occupancy of the molecular target, the potential pharmacologic effects of the tracer must be both safe and acceptable within the experimental paradigm. If these studies are not performed, B_{max} and K_d cannot be measured separately, and only their ratio ($BP = B_{max}/K_d$) is used as the outcome measure (21).

Methods to Measure Binding Potential

In vivo quantification has followed the well-established Law of Mass Action applied to ligand–receptor interactions under equilibrium conditions:

$$\frac{B}{F} = \frac{B_{max}}{K_d + F} \qquad [1]$$

where B is the concentration of radiotracer bound to the receptor and F is the concentration of free radiotracer (i.e., not bound to proteins) in the vicinity of the receptor. Because radiotracer imaging typically involves the injection of a miniscule mass dose of ligand, the concentration of free radiotracer is quite low. That is, $F << K_d$, with the result that

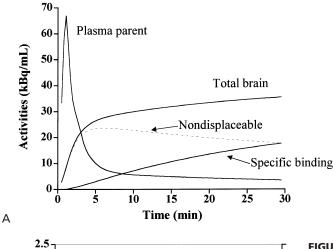$$\frac{B}{F} = \frac{B_{max}}{K_d} \qquad [2]$$

Thus, BP can be simply estimated as the equilibrium ratio of bound (B) to free (F). With this fairly standard three-compartment model (i.e., two tissue compartments and one blood compartment; Fig. 31.2), B is denoted as C_3 and F as f_1*C_1. Thus, $B/F = C_3/(f_1*C_1)$. This equation makes the reasonable assumption for drugs that pass blood–brain barrier by passive diffusion that the concentration of free tracer in plasma (f_1*C_1) equals that in brain under equilibrium conditions. Note that Eqs. 1 and 2 refer to *equilibrium* binding conditions. Following the bolus injection of tracer, the ratio of receptor-bound tracer (B) and free tracer (F) changes dramatically and is not under equilibrium conditions. Figure 31.4 provides a schematic representation of radiotracer concentrations in brain and plasma following a bolus injection with Fig. 4A showing early time points and Fig. 4B showing the entire data. With use of the complete time–activity curves from brain (measured with a PET or a SPECT camera) and arterial plasma (directly sampled and measured in a gamma counter), the goal of compartmental modeling is to estimate the ratio of B and F under *equilibrium* conditions. In other words, if the free level could be maintained at a constant level, how many times higher than the free level (F) would the concentration of receptor-bound tracer (B) finally and stably be?
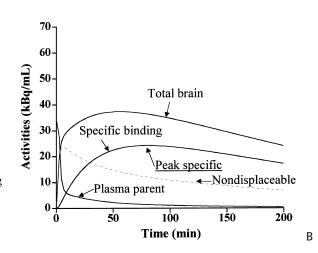
Several methods to estimate receptor parameters have been applied in radiotracer imaging and are briefly summarized below.

1. Compartmental modeling. Often viewed as the "gold standard," compartmental modeling typically requires concurrent and lengthy measurements of parent compound (separated from radioactively labeled metabolites) in plasma and of the brain time–activity curve. Kinetic parameters (K_1, k_2, k_3, k_4) are estimated from this so-called arterial input function (i.e., C_1) and the "impulse response function" of the brain (i.e., sum of C_2 and C_3). The goal of compartmental modeling is to determine the values of the rate constants between these compartments (Fig. 31.2), which when applied to the measured values of C_1 generate a brain time–activity curve similar to that actually measured with the PET or SPECT camera. The underlying concept is that the equilibrium ratio of B and F is equal to a ratio of kinetic rate constants.

$$BP = \frac{B_{max}}{K_d} = \frac{K_1 \bullet k_3}{k_2 \bullet k_4 \bullet f_1}$$

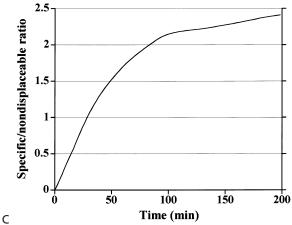The major disadvantage of kinetic analysis of compart-

A

B

C

FIGURE 31.4. **A,B:** Simulated time–activity curves of parent tracer in plasma and compartments in brain, and **(C)** ratio of specific to nondisplaceable uptake. The plasma parent curve was created by the following formula:

$$C_1\,(t) = \sum_{i=1}^{3} A_i \exp\left\{-\frac{(t-1)\ln 2}{T_i}\right\}$$

where A_1, A_2, and A_3 were 60, 5, and 2 kBq/mL, respectively, and T_1, T_2, and T_3 were 1, 20, and 100 minutes, respectively. A linear increase of the input curve was assumed between 0 and 1 minute. The curves of brain compartments were created with the rate constants $K_1 = 0.2$, $k_2 = 0.03$, $k_3 = 0.04$, and $k_4 = 0.02$ min^{-1}. The ratio of specific to nondisplaceable uptake gradually increases and reaches the equilibrium value 2 ($= k_3/k_4$) **(C)**. This time point is almost equal to the time when specific uptake reaches to the maximum value (time of peak equilibrium) **(B)**. After this time point, the ratio of specific to nondisplaceable uptake shows a further increase, which indicates that an equilibrium value of 2 can be obtained at only one time point.

mental modeling may often be logistic in nature because arterial sampling may be poorly tolerated, measurement of parent radiotracer in plasma may be technically difficult, and prolonged periods of data acquisition may be needed for both plasma and brain activities. The subsequent methods were developed in large part as "simpler" techniques to obtain receptor measurements that closely correlate with or directly equal those obtained in a complete compartmental analysis.

2. Peak equilibrium method. Based on good theoretic grounds, the "peak equilibrium method" [commonly attributed to Farde et al. (19) for radiotracer imaging] selects a unique equilibrium time as that when specific binding achieves its maximal level. Specific binding is operationally defined as activity in a target region (e.g., striatum) minus that in a background tissue region (e.g., cerebellum). From a practical perspective, a subject is continuously imaged for an hour or two following a bolus injection of tracer. Activities in target and background regions are plotted, and specific binding is calculated at each time point as the difference of the two curves (Fig. 31.4B). At the time of peak specific activity, a measure proportional to binding potential is cal-

culated as specific/nondisplaceable = (target − background)/background, as in (striatum − cerebellum)/cerebellum for a D2 tracer.

One major advantage of the peak equilibrium method is that plasma measurements are not required. Its major limitations include the following:

(a) Background activity in brain is proportional but not equal to the free level of tracer (*F*). Thus, the outcome measure is not equal to *BP*; rather this ratio of specific to nondisplaceable uptake is proportional to *BP*.

(b) Nonspecific binding in the background region may not equal that in the target region, a situation that can be caused, for example, by different proportions of white and gray matter in the two regions. The assumption of equivalent nonspecific binding has been evaluated (usually in animals) with displacement of radiotracer binding by high doses of a nonradioactive drug that also binds to the site. The assumption would be supported by equivalent levels of residual activities in target and background regions with complete receptor blockade.

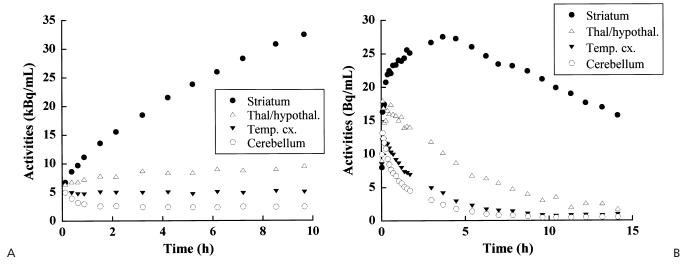(c) The time curves of free levels in target and background regions would be predicted not to overlap exactly.

FIGURE 31.5. Brain time–activity curves in a bolus plus constant infusion/equilibrium **(A)** and a bolus/kinetic study **(B)** of [^{123}I]epidepride. **A:** [^{123}I]Epidepride was given as a bolus (145 MBq) followed by constant infusion with bolus/infusion ratio of 6.0 hours (the amount of the tracer given for 6 hours by constant infusion was equal to that of the bolus) in a 33-year-old man. Note that equilibrium was achieved only in low-density regions (thalamus/hypothalamus and temporal cortex), not in a high-density region (striatum), with this bolus/infusion ratio. To achieve equilibrium in all regions, including striatum, a higher bolus/infusion ratio and longer infusion are required. **B:** [^{123}I]Epidepride (371 MBq) was give as a bolus to a 24-year-old man. (Part **B** reprinted from Fujita M, et al. Kinetic and equilibrium analyses of [^{123}I]epidepride binding. *Synapse* 1999; 34:290–304, with permission.)

For example, during the uptake portion of the curve, the free level would be lower in the target region because both receptors and nonspecific sites bind the tracer. Thus, at the time of peak specific uptake, the free level in the target region would not be the same as that in the background region. Depending on the kinetics of specific and nonspecific binding, the resulting discrepancy might be significant.

3. Constant infusion methods. Stable levels of drugs, including radiotracers, can be achieved with constant (sometimes called *continuous*) intravenous infusion of the drug (Fig. 31.5A). At some point, typically referred to as *steady state,* the amount of drug entering the blood will equal that leaving the vascular compartment. The levels of both total and free drug in plasma will subsequently be stable. At a somewhat later time point, the amount of drug binding to a receptor in an organ will equal that coming off the receptor; the level of receptor-bound drug will subsequently be stable. In an analogy to *in vitro* receptor binding studies, this stable condition is a state of equilibrium receptor binding.

The constant infusion (or so-called equilibrium) method is computationally much simpler than compartmental modeling and does not require extensive brain imaging or arterial plasma measurements. The concentration of receptor-bound tracer (*B*) can be estimated as target minus background. The level of free tracer in plasma (*F*) can be measured in either venous or arterial plasma because the body as a whole is in a condition of steady state. From a practical

perspective, the subject is connected to an intravenous pump for several hours, and then a single image is acquired (e.g., 30-minute duration) and a single venous blood sample is obtained. The major disadvantage of this technique is that many hours of infusion may be required to achieve steady-state conditions in both plasma and brain. In addition, data are acquired during a relatively short interval (e.g., 30 minutes) of a long infusion period (e.g., 7 hours). Thus, activity measurements before and after the relatively brief acquisition are not used, and the resulting radiation exposure to the subject can be viewed as "wasteful." In contrast, "all" activity is measured and used in the analysis of a bolus/kinetic study (Fig. 31.5B). From a practical perspective, the total amount of injected activity is often fairly equivalent for a bolus/kinetic and a constant infusion/equilibrium study. However, the total activity in brain after many hours of decay may be quite low and cause statistical counting errors.

In summary, three basic methods can be used to estimate receptor binding potential: (a) compartmental analysis of a bolus/kinetic study, (b) peak equilibrium, and (c) equilibrium imaging following constant infusion of the tracer (with or without an initial bolus of tracer). For all three methods, the target parameter is typically B_{max}/K_d, which equals the equilibrium value of B/F under tracer occupancy conditions (i.e., < 10% of the receptor occupied by tracer). The "true" binding potential (B_{max}/K_d) can be calculated if the free concentration of tracer in plasma is measured with the as-

sumption that free concentration in plasma equals that in brain. In this case, the measurement of *BP* is the ratio of receptor-bound activity in brain to free plasma activity (*F*). Because a blood sample is not used in the peak equilibrium method, the true *BP* cannot be measured. An alternate outcome measure for each of these three methods uses the non-displaceable activity in a background region of brain as a value proportional to free tracer concentration. This so-called poor man's binding potential is a ratio of activities in different regions of the brain (specific to nondisplaceable), and therefore plasma measurements are not required.

ESTIMATION OF ENDOGENOUS NEUROTRANSMITTER LEVELS

Molecular imaging probes can be used not only to measure a specific target but also, under appropriate conditions, to estimate concentrations of endogenous compounds that compete with the tracer for binding to the target. For example, a D2-receptor probe can be used not only to measure D2 receptors but also the extent of competition of this binding caused by endogenous dopamine. In fact, the most extensively studied indirect measurements have been the interaction of dopamine with D2-receptor ligands. These studies are briefly reviewed, and the special characteristic of a good ligand for such indirect measurements are discussed.

Tonic and Phasic Release of Dopamine

Dopamine transmission in striatum is thought to occur in two different modes, tonic and phasic (22,23). Tonic dopamine release represents the steady-state level of dopamine in the extracellular space, which is estimated to be in the nanomolar range. On the other hand, in phasic release, high extracellular concentrations of dopamine (millimolar range) are released within or near a synapse during an action potential. Close relationships have been proposed between abnormalities in phasic and tonic dopamine release and the symptoms of schizophrenia. Namely, excessive phasic release causes psychosis, and decreased tonic release causes cognitive deficits and negative symptoms (24).

Phasic release has typically been initiated by intravenous administration of a stimulant such as amphetamine or methylphenidate. These agents elevate synaptic dopamine concentrations either by releasing dopamine in a reverse manner via a dopamine transporter (amphetamine) or by blocking dopamine transporter-mediated reuptake of dopamine (methylphenidate). In an imaging study, the elevation of synaptic dopamine levels is estimated by the decrease in D2 radiotracer binding following stimulant administration in comparison with control conditions. Just as careful quantification is required for direct radiotracer binding to a molecular target, a similar if not even more rigorous approach is required for these indirect methods to ensure that mea-

surements of both the tracer and the competing displacer represent "equilibrium" values and not just transient pharmacokinetic "artifacts." To support the validity of these measurements, microdialysis studies have been performed in conjunction with D2-receptor imaging and a stimulant challenge (25,26). Although D2-ligand displacement correlated with the increase in extracellular dopamine measured with microdialysis, the relative increase in extracellular dopamine (1,000% to 4,000%) was much greater than the percentage of displacement of the ligand binding (5% to 15%). Thus, D2-receptor displacement is a "low-gain" monitor (i.e., underestimation) of the increase in extracellular dopamine. The reasons that the changes in binding are so much lower (although still, it is hoped, linear) relative to the increase in extracellular dopamine are unclear. This "low-gain" monitoring may reflect the fact that the imaging measurements cannot temporally track and therefore lag behind the chemical changes they are designed to measure. In other words, the displacement of radiotracer from the brain region occurs over a much slower time course than the relatively rapid changes in extracellular dopamine. Nevertheless, these stimulant-induced displacement studies appear to provide some reflection of changes in synaptic dopamine levels because they are relatively well correlated and because depletion of tissues levels of dopamine can block the effects of amphetamine (27).

The tonic release of dopamine has been estimated by the increase in D2-receptor binding induced by the depletion of endogenous dopamine. The removal of dopamine "unmasks" receptors, which then become available for radiotracer binding. The percentage of unmasking reflects the percentage of D2 receptors occupied by dopamine under basal or tonic conditions. Dopamine depletion has been induced in both animals and humans, with a resulting increase in D2 radiotracer binding (28,29). One limitation of these studies, especially in humans, is the difficulty of knowing whether depletion is essentially complete, so that the full extent of dopamine occupancy of the receptor has been measured. For example, if differences in unmasking are found in two subjects, does that reflect different levels of endogenous dopamine—or just different levels of dopamine depletion? A second limitation of this depletion paradigm is that increased receptor binding may not reflect "unmasking" but rather an up-regulation of D2-receptor levels, similar to that often found in denervation supersensitivity. One mechanism to minimize this potential confound is to perform the measurements as soon after dopamine depletion as possible. However, one clear advantage of the depletion paradigm in comparison with the stimulant-induced increase is that the depleted levels can typically be stably maintained during the scan. Thus, the relative slowness of the imaging measurements does not present a pharmacokinetic confound, as it does in studies with stimulant-induced release of dopamine.

Both stimulant and depletion studies have been performed in patients with schizophrenia. In general agreement

with the hypothesis of Grace, the "phasic" increase in synaptic dopamine (assessed following amphetamine administration) has been found to be elevated in drug-free schizophrenic patients, and the decrease in D2 radiotracer binding correlates with a transient increase in psychotic symptoms (30–32). In addition, stimulant depletion studies have found greater unmasking of striatal D2 receptors in patients with schizophrenia, which suggests that basal/tonic synaptic dopamine levels are higher in this disorder (33).

Affinity of Radiotracer

The relationship between affinity of the radiotracer and the sensitivity of its binding to endogenous dopamine is a source of confusion. Under *in vitro* equilibrium conditions and at tracer levels of radioactively labeled ligand, both the Michaelis–Menten and Cheng–Prusoff equations predict that the percentage of receptor occupancy by a competitive inhibitor (e.g., dopamine or other neurotransmitters) depends on the affinity of the inhibitor for the receptor and is independent of the affinity of the radioactively labeled ligand. However, such equilibrium binding conditions are achieved for neither the tracer nor the displacer if each is injected as a bolus. Even under these conditions, the sensitivity of radioligand binding to endogenous dopamine levels is theoretically (at least based on the *in vitro* theories) independent of the affinity of the radioactively labeled ligand when both the tracer and the displacer have achieved equilibrium binding conditions. However, if either the radiotracer (as in the bolus injection paradigm) or endogenous dopamine (as in stimulant-induced release) changes dynamically over time, the equilibrium condition is not achieved, and the apparent sensitivity of the radioligand to endogenous dopamine levels is determined by the kinetic properties of the radioligand (34,35). Equilibrium conditions can be achieved for both tracer and displacer in the dopamine depletion paradigm. For example, equilibrium can be achieved with bolus plus constant infusion of the radiotracer, and stable dopamine depletion with AMPT (α-methyl-*p*-tyrosine). The high-affinity D2 radioligand [123I]epidepride provides an instructive example of the differences seen in kinetic and equilibrium studies. The kinetics of its uptake in brain are slow and do not show displacement by transiently increased dopamine levels induced with amphetamine (36). However, stable low levels of dopamine induced with AMPT show unmasking of D2 receptors (37).

In Vivo Confounding Factors

Although the displacement of radioligand binding by neurotransmitter can be simply described with *in vitro* tissue homogenates, several factors complicate the interpretation of *in vivo* experimental results. (a) The affinity states of some receptors for agonists, but not antagonists, is regulated by the receptor to guanyl nucleotide-binding proteins (38).

Therefore, *in vivo* measurements are influenced by the affinity states and agonist or antagonist properties of the radiolabeled tracer, and results obtained with agonist and antagonist tracers may be different. (b) Agonist binding typically causes receptor internalization of G protein-coupled receptors (39,40). Thus, the endogenous agonist dopamine presumably facilitates the intracellular trafficking of D2 receptors (41), and radiotracers may differ in their affinity for the internalized versus membrane-bound receptor. (c) A significant proportion of D2 receptors are located extrasynaptically (42,43), where the concentration of dopamine is lower than in the synapse. Thus, neurotransmitters may occupy a smaller percentage of extrasynaptic receptors than of receptors within the synapse, and the *in vivo* measurement may not truly reflect synaptic neurotransmitter levels.

INTERACTION AMONG NEUROTRANSMISSION SYSTEMS

Abnormalities in psychiatric disorders likely represent the complex interaction of several neurotransmitter systems in the brain. PET imaging has recently been used to examine aspects of neurotransmitter interactions. For example, Dewy and colleagues (44–46) have pioneered studies on interactions among dopamine, GABA, and acetylcholine (ACh) systems in striatum. GABA neurons in the striatum have inhibitory effects on nigral dopamine neurons, nigral dopamine neurons have inhibitory effects on striatal ACh neurons, and striatal ACh neurons have facilitating effects on striatal GABA neurons. By estimating dopamine levels in striatum as described above, Dewey and collaborators showed in human or anesthetized nonhuman primates that the blockade of cholinergic transmission by benztropine (44) or scopolamine (45) decreased [11C]raclopride binding (increase in dopamine levels) and that stimulation of GABAergic transmission by γ-vinyl-GABA (a suicide inhibitor of GABA transaminase) and lorazepam (a benzodiazepine agonist) increased [11C]raclopride binding (decrease in dopamine levels) (46). In addition, they showed that a dopamine antagonist, *N*-methylspiroperidol, induced a decrease in [*N*-11C-methyl]benztropine binding, indicating an increase in ACh levels (44).

Other interactions have also been studied with PET. In two human studies, an *N*-methyl-D-aspartate (NMDA) antagonist, ketamine, decreased [11C]raclopride binding in striatum (47,48). In two human studies with similar techniques, the binding of [11C]raclopride was decreased by stimulation of 5-hydroxytryptamine (5-HT) transmission with fenfluramine (a 5-HT releaser) (49) or psilocybin (a mixed 5-HT$_{2A}$ and 5-HT$_{1A}$ agonist) (50). However, these results are discordant with those of previous studies in baboon, in which citalopram (a 5-HT uptake inhibitor) increased [11C]raclopride binding (51). Key aspects of the interaction between dopamine and 5-HT neurotransmitter

systems may well be mediated by glutamate. One significant limitation of these studies is that no useful glutamatergic PET probes have been developed to examine this important mediating neurotransmitter system. Furthermore, the linkage of pharmacologic challenges can be difficult to interpret. For example, if a disorder is associated with an abnormal dopamine outcome measured with PET in response to a 5-HT challenge, is the abnormal response caused by altered sensitivity of the dopamine or 5-HT system?

The results of these studies of interactions among neurotransmission systems have been interpreted under a simple assumption that the binding of [11C]raclopride and other tracers is affected by synaptic neurotransmitter levels. This simple assumption has been questioned by elaborate studies by Tsukada et al. (52). They measured dopamine synthesis, dopamine transporter, and dopamine D2 receptor with L-[β-11C]methyldopa (L-[β-11C]DOPA), [11C]β-CIT, and [11C]raclopride, respectively, in combination with microdialysis in conscious rhesus monkeys. Scopolamine did not change extracellular dopamine levels in the striatum but increased [11C]raclopride binding by decreasing its affinity at the dopamine D2 receptor (52) Furthermore, ketamine decreased [11C]raclopride binding in the striatum without increasing extracellular dopamine levels, and it increased both dopamine synthesis and dopamine availability (53).

Although interpretation may be difficult, and although the pharmacokinetics of either the tracer or displacer and changes in the synthesis and reuptake of neurotransmitters and affinity of receptor binding may complicate the experiment, the authors feel that challenges linked with radiotracer imaging are likely to provide useful information to allow a better understanding of the pathophysiology of neuropsychiatric disorders.

USE OF RADIOTRACER IMAGING IN THERAPEUTIC DRUG DEVELOPMENT

Radiotracer imaging can provide useful information about molecules that are either the direct target of or indirect markers for the effects of therapeutic drugs. For example, if both the tracer and therapeutic drug competitively bind to the same target, then imaging can provide direct information on the extent and kinetics of receptor occupancy in the relevant tissue. In addition, the molecular target measured by the tracer (e.g., amyloid) can be used as a "surrogate" biological marker to assess the efficacy of the therapeutic agent (e.g., one designed to decrease amyloid deposition).

Measurement of Receptor Occupancy

Molecular imaging can provide useful guidance for two aspects of drug administration: dose and dosing interval. The dose is most easily chosen with a known target occupancy

and accepted range. For example, typical antipsychotic agents occupy 50% to 80% of striatal D2 receptors (54). Thus, a new typical antipsychotic agent should show a reasonably acceptable side effect profile when given at doses that occupy this range of D2 receptors. With regard to dosing interval, the drug may be retained in tissue much longer than in plasma, and, therefore dosing intervals based on plasma pharmacokinetics may be too frequent. Such a situation has clearly been shown for antipsychotic agents, with which a high rate of receptor occupancy extends well beyond low plasma levels (55,56).

The measurement of receptor occupancy and pharmacokinetics in brain combined with the evaluation of adverse reactions in a small number of healthy subjects may provide valuable information for "go/no go" decisions at early stages of clinical drug development. If targeted receptor occupancy is achieved without causing adverse reactions, studies in patients are justified. If not, further studies may not be indicated. Even in the absence of a target level for receptor occupancy, it is reasonably safe to assume that doses associated with greater than 95% occupancy are unnecessarily high, and that those with less than 10% occupancy are unlikely to be efficacious.

The 5-HT$_{2A}$ antagonist M100907 may provide the best example of the use of PET receptor occupancy to provide useful information on dose and dosing interval. By measuring receptor occupancy with [11C]*N*-methylspiperone in healthy human subjects, initially an appropriate amount of a single dose (57) and then an appropriate dose and dosing interval were determined (56). Further, a similar level of receptor occupancy was recently confirmed with [11C]M100907 in a small number of patients with schizophrenia (58).

Dopamine Transporter Imaging as a Biological Marker in Parkinson Disease

Imaging of a biological marker may provide information that is useful either for diagnosis or as a monitor of disease progression. In Parkinson disease, the two most successful imaging targets used as biological markers are measures of dopamine synthesis with [18F]FDOPA and of dopamine terminal innervation with ligands for dopamine transporter.

The symptoms of Parkinson disease are caused by the progressive loss of dopamine neurons in the nigrostriatal pathway. Therefore, a reasonable method of diagnosis would be to "count" the number of dopamine neurons noninvasively. Such measurements are possible with *in vivo* imaging tracers: [18F]FDOPA and various SPECT/PET tracers for dopamine transporter. However, these tracers do not detect the same biological process. Whereas [18F]FDOPA detects metabolic activities at dopamine nerve terminals, the tracers for dopamine transporter simply measure the density of the target protein. Because of this difference, the sensitivity to detect the decrease in dopamine neu-

rons may be different. In fact, both human and animal studies have indicated that the imaging of dopamine transporter is more sensitive to dopamine neuronal loss (59). Dopamine transporter can be quantified with SPECT tracers, which can be used with lower cost than can PET studies. Therefore, imaging of the dopamine transporter in movement disorders is widely performed in many developed countries.

It is clinically important but sometimes difficult to differentiate essential tremor and Parkinson disease. Dopamine transporter imaging clearly distinguishes these two groups, with only a small overlap (60,61). However, dopamine transporter imaging is not able to distinguish idiopathic Parkinson disease from other parkinsonian syndromes, such as multiple system atrophy (62). Further, these techniques have shown bilateral loss of dopamine transporter in hemi-Parkinson disease (i.e., the earliest stage of the disorder), which suggests that even preclinical disease may be detected (63).

Restoring dopamine levels with L-DOPA is still the core medication treatment of Parkinson disease. However, long-term treatment with L-DOPA frequently results in fading of the therapeutic effect and the development of serious motor and psychiatric side effects. Although palliative treatment with L-DOPA is clearly of significant clinical benefit, current drug development is oriented toward neuroprotective treatments designed to slow the loss of dopamine neurons and the consequent progression of symptoms. As a biological marker of dopamine terminal innervation of the striatum, dopamine transporter imaging may well be useful to monitor whether such new therapies actually slow the loss of dopamine neurons. In fact, SPECT imaging is sensitive to and can quantify dopamine transporter loss in longitudinal studies of patients with Parkinson patients treated with conventional therapies (64–66). Therefore, with appropriate sample sizes, this imaging technique can quantify a relevant biological marker as a surrogate measure of the efficacy of putative neuroprotective therapies.

IMAGING POST-RECEPTOR SIGNAL TRANSDUCTION

The majority of the imaging studies performed to date have focused on the synapse: transporters as presynaptic targets, receptors as postsynaptic targets, and indirect measurements of the transmitter as a type of "intrasynaptic" target. However, measurements of membrane receptors merely "scratch the surface" of the cell and ignore the multitude of important intracellular mechanisms required for biological effects. Therefore, two promising areas for expansion in the near future are post-receptor signal transduction and subsequent changes in gene expression. Abnormalities in second messenger systems have been postulated to play important pathophysiologic roles in many psychiatric illnesses, includ-

ing mood disorders (67) and drug addiction (68). However, only a small number of PET and SPECT studies have been performed on these systems. Although tracers have been developed to image three major biochemical cascades [i.e., cyclic adenosine monophosphate (cAMP), phosphoinositide (PI), and arachidonate pathways], all existing ligands have moderate to significant technical limitations, and better ones are clearly needed. Some of these tracers are lipids, and their nonspecific binding is too high. In addition, because most of these tracers do not bind to a single type of protein but are metabolized by several enzymes, the interpretation of the results is not clear.

cAMP Cascade

Imaging of this signal transduction system was initially attempted by labeling its activator, forskolin, and a related analogue, 1-acetyl-7-deacetylforskolin, with ^{11}C (69,70). The binding of [^{11}C]forskolin may be correlated with the activation of adenylate cyclase (71). However, brain uptake of these tracers is very low (69).

Recently, imaging of this cascade was tried with an inhibitor of phosphodiesterase IV (PDE-IV), [^{11}C]rolipram (72). PDE-IV is the major subtype in brain of PDE, which hydrolyzes cAMP into 5′-AMP. PDE-IV is composed of four major enzyme subtypes, PDE-IV A, B, C, and D, and all four subtypes are found in human brain (73). Rolipram binds to and inhibits all four PDE-IV subtypes with high affinity. In one report of a rat *ex vivo* study, [^{11}C]rolipram was a promising tracer exhibiting high specific brain uptake (72). Further evaluation of the binding selectivity and kinetics must be performed in nonhuman primates and humans subjects.

Phosphoinositide System

Imahori and colleagues have studied the PI system *in vivo* using ^{11}C-labeled (74) and ^{123}I-labeled (75) 1,2-diacylglycerol. They showed specific incorporation of the tracer in the chemical components of the rat PI system, such as phosphatidic acid, phosphatidylinositol, phosphatidylinositol 4-phosphate, and phosphatidylinositol 4,5-*bis*-phosphate (74). Further, the tracer uptake was increased by an agonist at the muscarinic ACh receptor, which is known to be coupled with the PI system (74). However, absolute quantification of the tracer uptake is probably difficult because of the high lipophilicity. As explained above ("Required Properties of an *In Vivo* Tracer"), high lipophilicity causes a high level of binding to plasma components (protein and cell membranes), which reduces delivery of the tracer into brain. Under these circumstances, intersubject variability in the amount of tracer delivered to brain may be primarily determined by its binding to plasma components and not by neuronal activity of the PI system. If intersubject variability in f_1 (the free fraction of tracer in plasma) is noted, tracer

uptake cannot be compared among different subjects. Tracers with high lipophilicity and high binding to plasma components enter the brain slowly, and [^{11}C]diacylglycerol did indeed show such behavior (76). Further, whatever amount of a highly lipophilic tracer actually crosses the blood–brain barrier tends to exhibit a high rate of nonspecific binding. In summary, because of the difficulty in absolute quantification, the utility of this tracer as a quantitative measure may be significantly limited.

Arachidonate

The utility of [^{11}C]arachidonate to detect *in vivo* activity of phospholipase A$_2$ has been studied rigorously. After intravenous injection, [^{11}C]arachidonate is readily taken up ("pulse labeling") and incorporated into cerebral phospholipids and other stable brain compartments (77). By stimulating receptors that are linked to phospholipase A$_2$, probably via the PI pathway, the labeled phospholipids are catalyzed to generate arachidonate, and the regionally localized enhancement of phospholipid turnover increases the uptake of [^{11}C]arachidonate. The cholinomimetic arecoline has been shown to increase [^{14}C]arachidonate levels, and this effect can be blocked with a muscarinic ACh-receptor antagonist (78). For the quantification of the activity of this signal transduction system, the measurement should not be affected by cerebral blood flow. Chang et al. (79) showed that the uptake of [^{11}C]arachidonate is relatively flow-independent in monkeys. As with radioactively labeled diacylglycerol, high lipophilicity may be a significant limitation in absolute quantification. The potential dependence of brain uptake on the plasma free fraction may preclude between-subject studies, although within-subject experimental designs may still be valid (e.g., before and after pharmacologic challenge).

IMAGING REGULATION OF GENE EXPRESSION

Signal transduction initiated with presynaptic firing does not terminate with the interaction of a transmitter with its receptors and consequent second messenger generation. Instead, signal transduction may extend to the nucleus with alterations in gene expression. A well-known example is the induction of the protooncogene c-*fos* by receptor–ligand interactions (80). In fact, oncogenes encoding growth factors, membrane receptors, cytoplasmic and membrane-associated protein kinases, guanosine triphosphate-binding proteins (GTP), and transcription factors play important roles in signal transduction and altered gene expression. These genes and their cognate proteins will be important future targets for brain imaging. Much of what we know about these proteins in the central nervous system is derived from studies of cancer biology. Thus, imaging oncogenes and

their protein products is also an exciting target for nuclear oncologists, in part because they are pharmacophores for drug development. Several modalities are applied in cancer imaging, including (a) imaging oncogene products with radioactively labeled antibodies, (b) imaging messenger RNAs with labeled antisense oligonucleotides (81), (c) imaging reporter gene products with labeled reporter probes (82, 83), and (d) applying conventional techniques with labeled small molecules that bind to particular oncogene products.

Because the blood–brain barrier presents a special obstacle in neuroimaging, most techniques successfully used in cancer imaging are difficult to apply in brain imaging. For this reason, the first approach with antibodies is not possible in brain imaging unless the integrity of the blood–brain barrier is disrupted, as in the case of brain tumors. The second approach, in which antisense oligonucleotides are used, is also difficult because these multiply charged compounds do not cross the blood–brain barrier in any appreciable amount. To make radioactively labeled oligonucleotide probes pass the blood–brain barrier, complicated techniques are required, including the utilization of receptor-mediated transport (e.g., insulin and insulin-like growth factor) (84).

The third technique, the use of reporter probes, is being rigorously pursued, with possible applications in gene therapies. The best imaging example is the use of labeled thymidine analogues (e.g., 5-iodo-2′-fluoro-2′-deoxy-1-β-D-arabino-furanosyl-uracil) in cells expressing herpes simplex thymidine kinase. The probe is phosphorylated by the viral but not by mammalian thymidine kinases and is thereby trapped within the cell, as in the brain uptake of 2-deoxyglucose analogues (85). The basic idea is that gene expression can be monitored by radiolabeled substrate ("reporter probe"), which is metabolized by a transfected gene ("reporter gene") product and trapped in cells but not metabolized by endogenous enzymes of the host (82,83). A reporter gene can be different from a therapeutic gene as long as parallel levels of expression are expected by sharing a common promoter.

At the moment, imaging of reporter probes is used to detect expression only of exogenously introduced genes. Endogenous gene expression, which is interesting in psychiatric research, could be studied by using transgenes containing endogenous promoters fused to a reporter gene (83). A limitation of these techniques in brain imaging is that the widely used reporter probes, the radiolabeled substrates of herpes simplex type 1 thymidine kinase, do not show good permeability of the blood–brain barrier. This limitation can be overcome by using dopamine D2 receptor as a reporter gene and D2 ligands as reporter probes (86,87). Because the expression of functional D2 receptors may cause unwanted effects, further studies are being performed on the use of D2-receptor mutants, which are not coupled with intracellular signaling but still maintain binding affinity for D2 ligands.

Parkinson disease provides a useful example for gene therapy of a neuropsychiatric disorder (88). The concept of gene therapy for Parkinson disease has grown directly from the promising results obtained by grafting fetal dopamine-producing neurons. However, the limited availability and ethically controversial nature of the tissue source have restricted the utility of fetal grafts in this disorder. As an alternative, a relatively unlimited supply of homogenous, well-characterized viral vectors could theoretically be produced to deliver tyrosine hydroxylase, the rate-limiting enzyme in dopamine synthesis. Attempts have also been made in animal models to deliver neuroprotective or neurotrophic factors, such as superoxide dismutase and glial cell line-derived neurotrophic factor, to prevent continued degeneration of dopamine neurons. Similar techniques of gene therapy have been investigated in motor neuron degenerative diseases and Alzheimer disease. Reporter genes whose probes can cross the blood–brain barrier, such as D2 receptors, can monitor the expression of these transfected genes. On the other hand, dopamine release from the grafts could be monitored by a conventional technique utilizing competition of radioligand binding to D2 receptors, as described in the section on estimation of endogenous neurotransmitter levels. In fact, this technique of receptor displacement has been used to detect dopamine release in patients with embryonic nigral transplants (89).

The fourth approach, the relatively conventional one of imaging with small probes for relevant gene or oncogene protein products, is hampered by the development of useful and selective probes. As described in the section on the required properties of an *in vivo* tracer, it is difficult to fulfill all the requirements for a successful brain-imaging agent. However, once good imaging agents are developed, these targets can in general be imaged without the complicated techniques required in the other three modalities, described above. Many new anticancer agents are being developed, and a significant number of these agents target signal transduction systems, which may also play pathophysiologic roles in psychiatric disorders (90,91). For example, Ras farnesyltransferase is a target for cancer chemotherapy and potentially also for brain imaging. After post-translational modifications, including farnesylation, Ras binds to the cell membrane and transmits signals. Many inhibitors of Ras farnesyltransferase have been developed as anticancer medications (92). Among them, a recently developed agent has a high affinity (93) and may be used as a template from which brain imaging agents can be developed. In addition, a small molecule ligand for epidermal growth factor receptor has been labeled with ^{11}C and has shown brain uptake (94).

Rapid developments in molecular biology and the advent of gene-targeting techniques have enabled the study of individual genes in mice by means of *in vitro* experimental techniques. Recently developed animal-dedicated PET devices (e.g., "rat PET" and "microPET") achieve high resolution of about 2 mm and can now image these animals *in vivo*

(6). These imaging studies may make it possible to apply new findings in molecular biology to the study of patients with neuropsychiatric disorders in exciting ways.

CONCLUSIONS

Progress in molecular neurobiology has dramatically changed our understanding of psychiatric disorders. A significant proportion of these findings have been obtained from animal experiments and postmortem human studies. A major challenge for neuroimaging in future years will be to extended the application of these *in vitro* probes to *in vivo* imaging of patients. Radiotracer imaging with PET, and to a lesser extent with SPECT, is ideally suited for such *in vivo* applications because of its extraordinarily high sensitivity and improving anatomic resolution (now about 2 mm). This chapter has reviewed what is arguably the most difficult barrier to accomplishing *in vivo* molecular imaging—the development of useful and quantifiable tracers. The blood–brain barrier is a challenge to both the delivery of radiolabeled tracers and the quantification of brain uptake of the tracers. However, many successful tracers have been developed to date. These probes have largely been synthesized as analogues of agents active at synaptic transmission and have provided measures of presynaptic, postsynaptic, and even "intrasynaptic" targets. Relatively little progress has been made in measuring intracellular signal transduction or gene expression. These two areas are clearly important targets for future ligand development. By bridging new findings in molecular neuroscience and clinical studies, *in vivo* molecular imaging will likely contribute to a greater understanding of psychiatric pathophysiology and, it is hoped, enhance the development of improved pharmacotherapies.

REFERENCES

1. Nunn AD, Linder KE, Tweedle MF. Can receptors be imaged with MRI agents? *Q J Nucl Med* 1997;41:155–162.
2. Rothman DL, Petroff OA, Behar KL, et al. Localized 1H NMR measurements of gamma-aminobutyric acid in human brain *in vivo*. *Proc Natl Acad Sci U S A* 1993;90:5662–5666.
3. Michaelis T, Merboldt KD, Bruhn H, et al. Absolute concentrations of metabolites in the adult human brain *in vivo*: quantification of localized proton MR spectra. *Radiology* 1993;187:219–227.
4. Abi-Dargham A, Simpson N, Kegeles L, et al. PET studies of binding competition between endogenous dopamine and the D1 radiotracer [^{11}C]NNC 756. *Synapse* 1999;32:93–109.
5. Bendriem B, Townsend DW. Volume imaging tomographs. In: Bendriem B, Townsend DW, eds. *The theory and practice of 3D PET.* Dordrecht: Kluwer Academic, 1998;111–132.
6. Chatziioannou AF, Cherry SR, Shao Y, et al. Performance evaluation of microPET: a high-resolution lutetium oxyorthosilicate PET scanner for animal imaging. *J Nucl Med* 1999;40:1164–1175.

7. Schmand M, Eriksson L, Casey M, et al. Performance results of a new DOI detector block for a high resolution PET–LSO research tomograph HRRT. *IEEE Trans Nucl Sci* 1998;45:3000–3006.

8. Levin VA. Relationship of octanol/water partition coefficient and molecular weight to rat brain capillary permeability. *J Med Chem* 1980;23:682–684.

9. Rowley M, Kulagowski JJ, Watt AP, et al. Effect of plasma protein binding on *in vivo* activity and brain penetration of glycine/NMDA receptor antagonists. *J Med Chem* 1997;40:4053–4068.

10. Dishino DD, Welch MJ, Kilbourn MR, et al. Relationship between lipophilicity and brain extraction of C-11-labeled radiopharmaceuticals. *J Nucl Med* 1983;24:1030–1038.

11. Kessler RM, Ansari MS, de Paulis T, et al. High-affinity dopamine D2 receptor radioligands. 1. Regional rat brain distribution of iodinated benzamides. *J Nucl Med* 1991;32:1593–1600.

12. Schlyer DJ, Volkow ND, Fowler JS, et al. Regional distribution and kinetics of haloperidol binding in human brain: a PET study with [^{18}F]haloperidol. *Synapse* 1992;11:10–19.

13. Fowler JS, Volkow ND, Wolf AP, et al. Mapping cocaine binding sites in human and baboon brain *in vivo. Synapse*1989;4: 371–377.

14. Kornhuber J, Schultz A, Wiltfang J, et al. Persistence of haloperidol in human brain tissue. *Am J Psychiatry* 1999;156:885–890.

15. Osman S, Lundkvist C, Pike VW, et al. Radioactive metabolites of the 5-HT$_{1A}$ receptor radioligand, [*O*-methyl-^{11}C]WAY-100635, in rat, monkey and humans plus evaluation of the brain uptake of the metabolite, [*O*-methyl-^{11}C]WAY-100634, in monkey. *J Label Compound Radiopharm* 1995;37:283.

16. Pike VW, McCarron JA, Lammerstma AA, et al. Exquisite delineation of 5-HT$_{1A}$ receptors in human brain with PET and [carbonyl-^{11}C]WAY-100635. *Eur J Pharmacol* 1996;301:R5–R7.

17. Huang S-C, Phelps ME. Principles of tracer kinetic modeling in positron emission tomography and autoradiography. In: Phelps M, Mazziotta J, Schelbert H, eds. *Positron emission tomography and autoradiography: principles and applications for the brain and heart.* New York: Raven Press, 1986:287–346.

18. Carson RE. Parameter estimation in positron emission tomography. In: Phelps ME, Mazziotta JC, Schelbert HR, eds. *Positron emission tomography and autoradiography: principles and applications for the brain and heart.* New York: Raven Press, 1986: 347–390.

19. Farde L, Eriksson L, Blomqvist G, et al. Kinetic analysis of central [^{11}C]-raclopride binding to D2 dopamine receptors studied with PET—a comparison to the equilibrium analysis. *J Cereb Blood Flow Metab* 1989;9:696–708.

20. Delforge J, Pappata S, Millet P, et al. Quantification of benzodiazepine receptors in human brain using PET, [^{11}C]flumazenil, and a single-experiment protocol. *J Cereb Blood Flow Metab* 1995; 15:284–300.

21. Mintun MA, Raichle ME, Kilbourn MR, et al. A quantitative model for the *in vivo* assessment of drug binding sites with positron emission tomography. *Ann Neurol* 1984;15: 217–227.

22. Grace AA. Phasic versus tonic dopamine release and modulation of dopamine system responsivity: a hypothesis for the etiology of schizophrenia. *Neurosci* 1991;41:1–24.

23. Grace AA. Cortical regulation of subcortical systems and its possible relevance to schizophrenia. *J Neural Transm [Gen Sect]* 1993; 91:111–134.

24. Moore H, West AR, Grace AA. The regulation of forebrain dopamine transmission: relevance to the pathophysiology and psychopathology of schizophrenia. *Biol Psychiatry* 1999;46:40–55.

25. Endres CJ, Kolachana BS, Saunders RC, et al. Kinetic modeling of [^{11}C]raclopride: combined PET–microdialysis studies. *J Cereb Blood Flow Metab* 1997;17:932–942.

26. Laruelle M, Iyer RN, al-Tikriti MS, et al. Microdialysis and SPECT measurements of amphetamine-induced dopamine release in nonhuman primates. *Synapse* 1997;25:1–14.

27. Innis RB, Malison RT, al-Tikriti M, et al. Amphetamine-stimulated dopamine release competes *in vivo* for [^{123}I]IBZM binding to the D2 receptor in nonhuman primates. *Synapse* 1992;0: 177–184.

28. Ross SB, Jackson DM. Kinetic properties of the accumulation of ^{3}H-raclopride in the mouse brain *in vivo. Naunyn Schmiedebergs Arch Pharmacol*1989;340:6–12.

29. Laruelle M, D'Souza C, Baldwin RM, et al. Imaging D2 receptor occupancy by endogenous dopamine in humans. *Neuropsychopharmacology* 1997;17:162–174.

30. Laruelle M, Abi-Dargham A, van Dyck CH, et al. SPECT imaging of amphetamine-induced dopamine release in drug-free schizophrenic subjects. *Proc Natl Acad Sci U S A* 1996;93: 9235–9240.

31. Breier A, Su TP, Saunders R, et al. Schizophrenia is associated with elevated amphetamine-induced synaptic dopamine concentrations: evidence from a novel positron emission tomography method. *Proc Natl Acad Sci U S A* 1997;94:2569–2574.

32. Abi-Dargham A, Gil R, Krystal J, et al. Increased striatal dopamine transmission in schizophrenia: confirmation in a second cohort. *Am J Psychiatry* 1998;155:761–767.

33. Abi-Dargham A, Kegeles L, Zea-Ponce Y, et al. Removal of endogenous dopamine reveals elevation of D2 receptors in schizophrenia. *J Nucl Med* 1999;40:30P(abst).

34. Morris ED, Fisher RE, Alpert NM, et al. *In vivo* imaging of neuromodulation using positron emission tomography: optimal ligand characteristics and task length for detection of activation. *Hum Brain Mapping* 1995;3:35–55.

35. Endres CJ, Carson RE. Assessment of dynamic neurotransmitter changes with bolus or infusion delivery on neuroreceptor ligands. *J Cereb Blood Flow Metab* 1998;18:1196–1210.

36. Al-Tikriti MS, Baldwin RM, Zea-Ponce Y, et al. Comparison of three high-affinity SPECT radiotracers for the dopamine D2 receptor. *Nucl Med Biol* 1994;21:179–188.

37. Fujita M, Verhoeff NPLG, Varrone A, et al. Imaging extrastriatal dopamine D2 receptor occupancy by endogenous dopamine in healthy humans. *Eur J Pharmacol* 2000;387:179–188.

38. Wreggett KA, Seemn P. Agonist high- and low-affinity states of the D2 dopamine receptor in calf brain. *Mol Pharmacol* 1983; 25:10–17.

39. Dumartin B, Caillé I, Gonon F, et al. Internalization of D1 dopamine receptor in striatal neurons *in vivo* as evidence of activation by dopamine agonists. *J Neurosci* 1998;18:1650–1661.

40. Ito K, Haga T, Lameh J, et al. Sequestration of dopamine D2 receptors depends on coexpression of G protein-coupled receptor kinases 2 or 5. *Eur J Biochem* 1999;260:112–119.

41. Chugani DC, Ackermann RF, Phelps ME. *In vivo* [^{3}H]spiperone binding: evidence for accumulation in corpus striatum by agonist-mediated receptor internalization. *J Cereb Blood Flow Metab* 1988;8:291–303.

42. Yung KK, Bolam JP, Smith AD, et al. Immunocytochemical localization of D1 and D2 dopamine receptors in the basal ganglia of the rat: light and electron microscopy. *Neuroscience* 1995;65: 709–730.

43. Khan ZU, Gutierrez A, Martin R, et al. Differential regional and cellular distribution of dopamine D2-like receptors: an immunocytochemical study of subtype-specific antibodies in rat and human brain. *J Comp Neurol* 1998;402:353–371.

44. Dewey SL, Brodie JD, Fowler JS, et al. Positron emission tomography (PET) studies of dopaminergic/cholinergic interactions in the baboon brain. *Synapse* 1990;6:321–327.

45. Dewey SL, Smith GS, Logan J, et al. Effects of central cholinergic

blockade on striatal dopamine release measured with positron emission tomography in normal human subjects. *Proc Natl Acad Sci USA* 1993;90:11816–11820.

46. Dewey SL, Smith GS, Logan J, et al. GABAergic inhibition of endogenous dopamine release measured *in vivo* with ^{11}C-raclopride and positron emission tomography. *J Neurosci* 1992;12: 3773–3780.

47. Breier A, Adler CM, Weisenfeld N, et al. Effects of NMDA antagonism on striatal dopamine release in healthy subjects: application of a novel PET approach. *Synapse* 1998;29:142–147.

48. Smith GS, Schloesser R, Brodie JD, et al. Glutamate modulation of dopamine measured *in vivo* with positron emission tomography (PET) and ^{11}C-raclopride in normal human subjects. *Neuropsychopharmacology* 1998;18:18–25.

49. Smith GS, Dewey SL, Brodie JD, et al. Serotoninergic modulation of dopamine measured with [11C]raclopride and PET in normal human subjects. *Am J Psychiatry* 1997;154:490–496.

50. Vollenweider FX, Vontobel P, Hell D, et al. 5-HT modulation of dopamine release in basal ganglia in psilocybin-induced psychosis in man—a PET study with [11C]raclopride. *Neuropsychopharmacology* 1999;20:424–433.

51. Dewey SL, Smith GS, Logan J, et al. Serotoninergic modulation of striatal dopamine measured with positron emission tomography (PET) and *in vivo* microdialysis. *J Neurosci* 1995;15: 821–829.

52. Tsukada H, Harada N, Nishiyama S, et al. Cholinergic neuronal modulation alters dopamine D2 receptor availability *in vivo* by regulating receptor affinity induced by facilitated synaptic dopamine turnover: positron emission tomography studies with microdialysis in the conscious monkey brain. *J Neurosci* 2000;20: 7067–7073.

53. Tsukada H, Harada N, Nishiyama S, et al. Ketamine decreased striatal [11C]raclopride binding with no alterations in static dopamine concentrations in the striatal extracellular fluid in the monkey brain: multiparametric PET studies combined with microdialysis analysis. *Synapse* 2000;37:95–103.

54. Farde L, Nordstrom A-L, Wiesel F-A, et al. PET analysis of central D1 and D2 dopamine receptor occupancy in patients treated with classic neuroleptics and clozapine—relationship to extrapyramidal side effects. *Arch Gen Psychiatry* 1992;49: 538–544.

55. Nyberg S, Farde L, Halldin C. Delayed normalization of central D2 dopamine receptor availability after discontinuation of haloperidol decanoate. Preliminary findings. *Arch Gen Psychiatry* 1997;54:953–958.

56. Grunder G, Yokoi F, Offord SJ, et al. Time course of 5-HT$_{2A}$ receptor occupancy in the human brain after a single oral dose of the putative antipsychotic drug MDL 100,907 measured by positron emission tomography [published erratum appears in *Neuropsychopharmacology* 1998;19:161]. *Neuropsychopharmacology* 1997;17:175–185.

57. Andree B, Nyberg S, Ito H, et al. Positron emission tomographic analysis of dose-dependent MDL 100,907 binding to 5-hydroxytryptamine-2A receptors in the human brain. *J Clin Psychopharmacol* 1998;18:317–323.

58. Talvik-Lotfi M, Nyberg S, Nordström A-L, et al. High 5HT$_{2A}$ receptor occupancy in M100907-treated schizophrenic patients. *Psychopharmacology* 2000;148:400–403.

59. Stoof JC, Winogrodzka A, van Muiswinkel FL, et al. Leads for the development of neuroprotective treatment in Parkinson's disease and brain imaging methods for estimating treatment efficacy. *Eur J Pharmacol* 1999;375:75–86.

60. Asenbaum S, Pirker W, Angelberger P, et al. [123I]beta-CIT and SPECT in essential tremor and Parkinson's disease. *J Neural Transm* 1998;105:1213–1228.

61. Lee MS, Kim YD, Im JH, et al. ^{123}I-IPT brain SPECT study in essential tremor and Parkinson's disease. *Neurology* 1999;52: 1422–1426.

62. Varrone A, Marek KL, Jennings D, et al. [^{123}I]β-CIT SPECT imaging demonstrates reduced density of striatal dopamine transporters in Parkinson's disease and multiple system atrophy. *Mov Disord (in press)*.

63. Booij J, Tissingh G, Winogrodzka A, et al. Imaging of the dopaminergic neurotransmission system using single-photon emission tomography and positron emission tomography in patients with parkinsonism. *Eur J Nucl Med* 1999;26:171–182.

64. Booij J, Winogrodzka A, Bergmans P, et al. [I-123]-beta-CIT and [I-123]FP-CIT SPECT are useful methods to monitor progression of dopaminergic degeneration in early-stage Parkinson's disease. *J Nucl Med* 1999;40:28P(abst).

65. Seibyl JP, Innis RB, Early ML, et al. Baseline striatal dopamine transporter uptake measured with [I-123]β-CIT SPECT may predict the rate of disease progression in idiopathic Parkinson's disease. *J Nucl Med* 1999;40:27P(abst).

66. Marek K, Innis R, van Dyck C, et al. [123I]β-CIT SPECT imaging assessment of the rate of Parkinson's disease progression. *Neurology (in press)*.

67. Duman RS, Heninger GR, Nestler EJ. A molecular and cellular theory of depression. *Arch Gen Psychiatry* 1997;54:597–606.

68. Nestler EJ. Molecular neurobiology of drug addiction. *Neuropsychopharmacology* 1994;11:77–87.

69. Sasaki T, Enta A, Nozaki T, et al. Carbon-11-forskolin: a ligand for visualization of the adenylate cyclase-related second messenger system. *J Nucl Med* 1993;34:1944–1948.

70. Sasaki T, Furukata K, Iimori T, et al. 1-Acetyl-7-deacetylforskolin: a potential non-specific inactive analog of forskolin for estimation of its specific high-affinity binding and adenylyl cyclase stimulation *in vitro*. *Life Sci* 1995;57:1367–1373.

71. Nelson CA, Seamon KB. Binding of [3H]forskolin to solubilized preparations of adenylate cyclase. *Life Sci* 1988;42:1375–1383.

72. Lourenco CM, DaSilva JN, Warsh JJ, et al. Imaging of cAMP-specific phosphodiesterase-IV: comparison of [11C]rolipram and [11C]Ro 20-1724 in rats. *Synapse* 1999;31:41–50.

73. Engels P, Fichtel K, Lubbert H. Expression and regulation of human and rat phosphodiesterase type IV isogenes. *FEBS Lett* 1994;350:291–295.

74. Imahori Y, Fujii R, Ueda S, et al. Membrane trapping of carbon-11-labeled 1,2-diacylglycerols as a basic concept for assessing phosphatidylinositol turnover in neurotransmission process. *J Nucl Med* 1992;33: 413–422.

75. Ohmori Y, Imahori Y, Ueda S, et al. Radioiodinated diacylglycerol analogue: a potential imaging agent for single-photon emission tomographic investigations of cerebral ischaemia. *Eur J Nucl Med* 1996;23:280–289.

76. Matsumoto K, Imahori Y, Fujii R, et al. Evaluation of phosphoinositide turnover on ischemic human brain with 1-[1-11C]-butyryl-2-palmitoyl-rac-glycerol using PET. *J Nucl Med* 1999; 40:1590–1594.

77. Robinson PJ, Noronha J, DeGeorge JJ, et al. A quantitative method for measuring regional *in vivo* fatty-acid incorporation into and turnover within brain phospholipids: review and critical analysis. *Brain Res Rev* 1992;17:187–214.

78. DeGeorge JJ, Nariai T, Yamazaki S, et al. Arecoline-stimulated brain incorporation of intravenously administered fatty acids in unanesthetized rats. *J Neurochem* 1991;56:352–355.

79. Chang MC, Arai T, Freed LM, et al. Brain incorporation of [1-11C]arachidonate in normocapnic and hypercapnic monkeys, measured with positron emission tomography. *Brain Res* 1997; 755:74–83.

80. Morgan JI, Curran T. Role of ion flux in the control of c-*fos* expression. *Nature* 1986;322:552–555.

81. Hnatowich DJ. Antisense and nuclear medicine. *J Nucl Med* 1999;40:693–703.

82. Blasberg RG, Tjuvajev JG. Herpes simplex virus thymidine kinase as a marker/reporter gene for PET imaging of gene therapy. *Q J Nucl Med* 1999;43:163–169.

83. Gambhir SS, Barrio JR, Herschman HR, et al. Assays for noninvasive imaging of reporter gene expression. *Nucl Med Biol* 1999; 26:481–490.

84. Pardridge WM. Drug delivery to the brain. *J Cereb Blood Flow Metab* 1997;17:713–731.

85. MacLaren DC, Toyokuni T, Cherry SR, et al. PET imaging of gene expression. *Synapse* 1999;34:290–304.

86. MacLaren DC, Gambhir SS, Satyamurthy N, et al. Repetitive, non-invasive imaging of the dopamine D2 receptor as a reporter gene in living animals. *Gene Ther* 1999;6:785–791.

87. Ogawa O, Umegaki H, Ishiwata K, et al. *In vivo* imaging of adenovirus-mediated over-expression of dopamine D2 receptors in rat striatum by positron emission tomography. *Neuroreport* 2000;11:743–748.

88. Barkats M, Bilang-Bleuel A, Buc-Caron MH, et al. Adenovirus in the brain: recent advances of gene therapy for neurodegenerative diseases. *Prog Neurobiol* 1998;55:333–341.

89. Piccini P, Brooks DJ, Bjorklund A, et al. Dopamine release from nigral transplants visualized *in vivo* in a Parkinson's patient. *Nat Neurosci* 1999;2:1137–1140.

90. Buolamwini JK. Novel anticancer drug discovery. *Curr Opin Chem Biol* 1999;3:500–509.

91. Seymour L. Novel anti-cancer agents in development: exciting prospects and new challenges. *Cancer Treat Rev* 1999;25: 301–312.

92. Leonard DM. *Ras* farnesyltransferase: a new therapeutic target. *J Med Chem* 1997;40:2971–2990.

93. Njoroge FG, Taveras AG, Kelly J, et al. (+)-4-[2-[4-(8-chloro-3,10-dibromo-6,11-dihydro-5H-benzo[5, 6]cyclohepta[1,2-β]-pyridin-11(*R*)-yl)-1-piperidinyl]-2-oxo-ethyl]-1-piperidinecarboxamide (SCH-66336): a very potent farnesyl protein transferase inhibitor as a novel antitumor agent. *J Med Chem* 1998;41: 4890–4902.

94. Fredriksson A, Johnstrom P, Thorell JO, et al. *In vivo* evaluation of the biodistribution of ^{11}C-labeled PD153035 in rats without and with neuroblastoma implants. *Life Sci* 1999;65:165–174.